2 THEORY

This chapter looks at the theory behind the experimental techniques employed in this project.

2.1 RHEOLOGY

2.1.1 Introduction

Newton considered the relative viscosity at different parts of a fluid in a hypothesis published in 1687. Relative viscosity is a measure of the resistance to flow of a liquid. Figure 1 represents two parallel surfaces of area, A, containing a liquid subjected to shear. A constant shear stress is applied to the upper surface which allows it to move with a constant velocity, U. Within the gap a velocity gradient is created which is continuous across the velocity across the gap. At the bottom surface the velocity is zero (assuming there is no slip between the surface and the liquid). The shear stress, σ, necessary to produce the movement of the upper surface is the force per unit area (F/A) required.

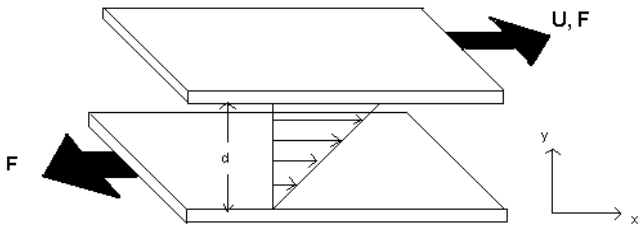

Figure 1. Diagram representing two surfaces held apart by a liquid that is subject to shear [1].

The shear stress (σ) can be related to the shear viscosity (η) and the shear rate (velocity gradient), U/d, using the following equation [1, 2]. Note that the shear rate is usually given the symbol, $\dot{\gamma}$.

$$\sigma = \eta\dot{\gamma}$$

Equation 2.1

This relationship is true for Newtonian fluids that can be characterised by the following [1]:

- The shear viscosity does not vary with shear rate (horizontal line for viscosity vs. shear rate plot).
- The viscosity is constant during the time of shearing and the stress in the fluid falls to zero when the shearing is stopped. In any subsequent shearing, however long the period of resting between measurements, the viscosity is as previously measured.
- The viscosities measured in different deformation are always in simple proportion to one another, e.g. the viscosity measured in a uniaxial extensional flow is always three times the value measured in simple shear flow.

Any deviations from these characteristics mean that the fluid is non-Newtonian, where viscosity is a function of shear rate as opposed to a constant coefficient. For non-Newtonian fluids, the shear viscosity can be represented by $\eta(\dot{\gamma})$ and so the relationship between shear stress and shear rate becomes:

$$\sigma = \eta(\dot{\gamma})\dot{\gamma}$$

Equation 2.2

If the fluid only breaks the first condition above then it can be termed a generalised Newtonian fluid, and the fluid can be shear thinning, shear thickening or a Bingham plastic.

For shear thinning fluids, the viscosity decreases with increasing shear rate, and for shear thickening the opposite is true, i.e. when the shear rate is increased the viscosity increases. Shear thickening fluids are rarer than shear thinning fluids, as suspensions, emulsions and polymers all tend to be shear thinning. From Figure 2 it can be seen that for fluids that are Bingham plastics, a critical shear stress value needs to be reached before they will flow.

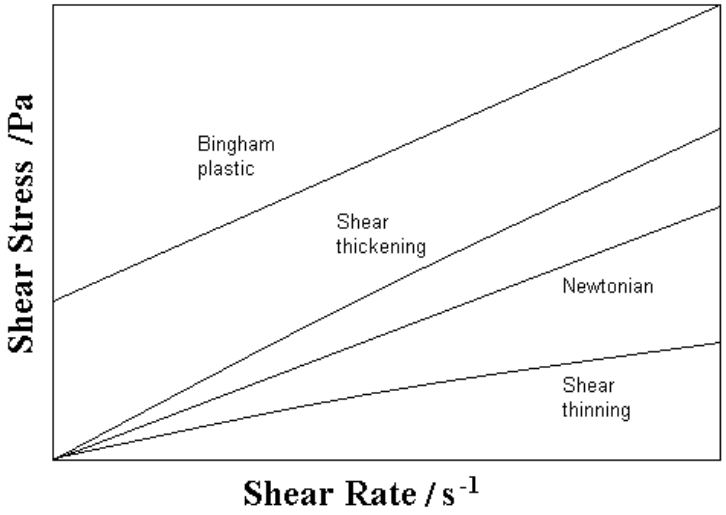

Figure 2. Plot of shear stress against shear rate for generalised Newtonian fluids [3].

2.1.2 Polymer Rheology

At the beginning of cure, epoxy resins are low molecular weight species that, like simple liquids, follow Newtonian behaviour where the viscosity is independent of the shear rate. If the polymerisation were to create linear polymers then the viscosity might be interpreted in terms of two regions. Initially, the viscosity is proportional to the molar mass of the material. As the cure proceeds, the molar mass increases until it reaches the critical molar mass M_c, which is the mass at which entanglement of the chains can occur. The cure continues above M_c and enters into non-Newtonian behaviour where the viscosity is now proportional to $M^{3.5}$ [4]. Figure 3 shows how the viscosity changes with increasing molar mass and highlights the critical molar mass M_c as point at which the two linear lines meet. At molar masses below M_c the system is Newtonian, and above M_c it is non-Newtonian as the effects of chain entanglement or reptation influence the behaviour. This value is therefore dependent on the chemical structure and flexibility of the particular system being studied. This type of behaviour is found for linear polymers which are not chemically crosslinked and would be typical of the effects observed for the polymerization of polystyrene. The behaviour of a multifunctional monomer such as an epoxy will be different.

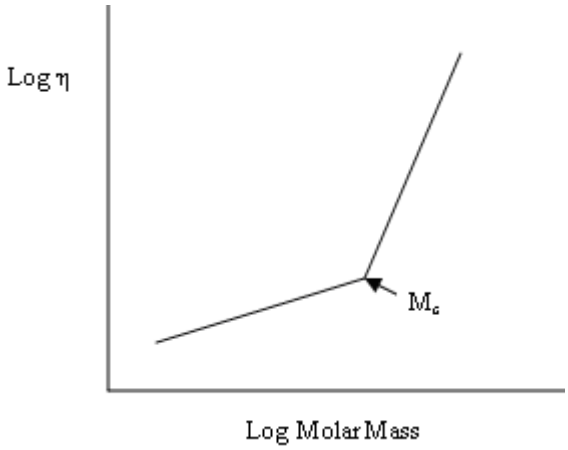

Figure 3. Plot showing change in viscosity as molar mass increases.

After initially producing pseudo linear polymers, epoxy resins then proceed to produce branched chain materials which will follow a different dependence on molar mass from that observed for linear polymers.

In order to understand in more detail the influence of polymer architecture on the viscosity it is necessary to explore the way in which the viscosity changes with shear rate. If the viscosity remains unchanged with increasing shear rate then the material is exhibiting Newtonian behaviour. As the molar mass increases then the viscosity increases, and shear thinning is observed.. Figure 4 shows how the viscosity varies with shear rate as the cure proceeds and molar mass increases, where the response for low molar mass is nearest to the x-axis, and each subsequent line is for increasing molar mass.

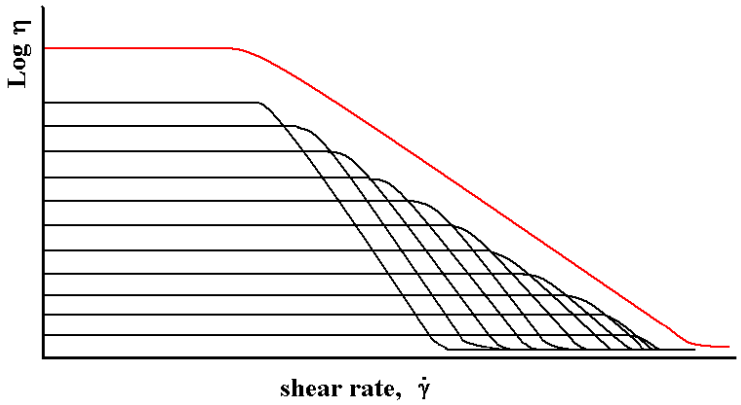

Figure 4. Plot showing change in viscosity with shear rate as cure proceeds, where the red line represents the highest cure time.

The shear dependence of a linear polymer which is entangled shows a profile which has two clear regions of shear thinning, as shown in Figure 5. The shear thinning at low shear rates is associated with the chains which are entangled attempting to become un-entangled.

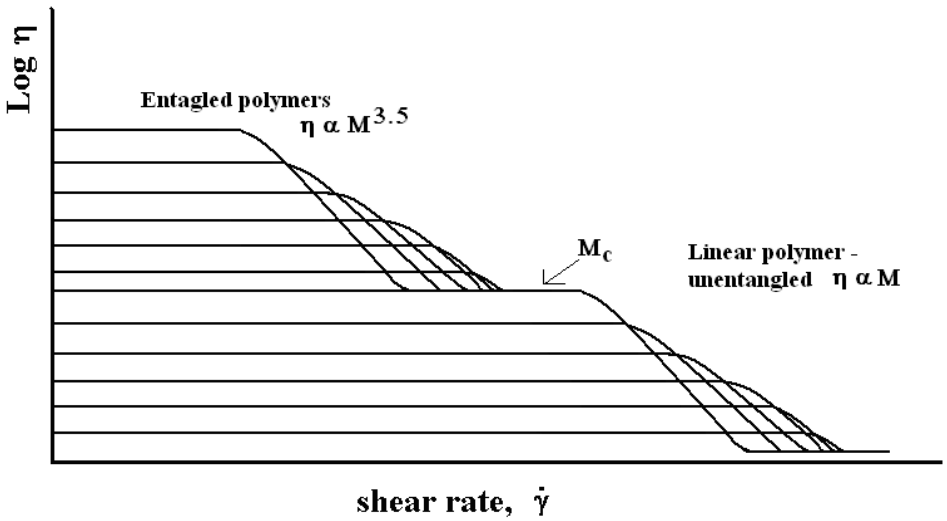

Figure 5. Plot showing change in viscosity with shear rate as cure proceeds - for polymers with molar mass above and below M_c.

When the low shear rate viscosity is plotted against the cure time, the viscosity is initially low when Newtonian behaviour is displayed. Viscosity then begins to rise quickly, as the molar mass increases and goes through the critical molar mass M_c [4]. This is displayed in Figure 6.

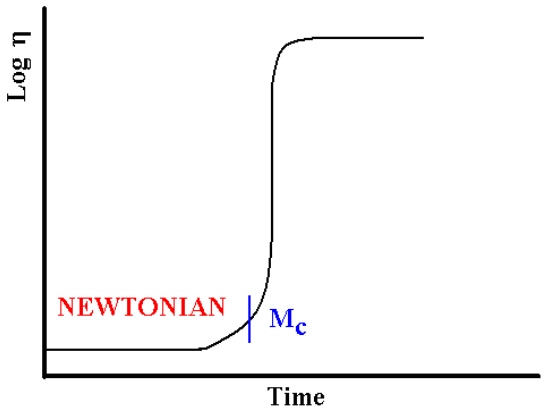

Figure 6. Plot of change in viscosity as cure time increases, with Newtonian region labelled.

2.1.3 Modelling of Polymer Behaviour

Figure 7 shows how viscosity varies with increasing shear rate in a concentrated polymer solution. At low shear rates, and low frequency, the motion of the polymer chains is predominantly diffusion controlled as the solvent that the polymer is dispersed in moves through the chains. This is associated with the zeroth mode, and the viscosity remains high and unaffected by the shear rate or frequency. The value is termed the low frequency limiting viscosity, η_0. It should be noted that shear rate is interchangeable with angular frequency in a simple polymer solution or melt.

As the shear rate is increased there comes a point when the two extremes of the chain are forced in opposite directions while the centre remains stationary. This centre is now termed a *node*, and the decreasing viscosity can be related to the first normal mode. See Figure 8 for a diagram of the nodes. As the shear rate is increased further, higher normal modes of relaxation are associated with the resultant decrease in viscosity, until a finite value is reached. This value is termed the high frequency limiting viscosity η_∞, and is the effective viscosity of the solvent that the polymer is dispersed in.

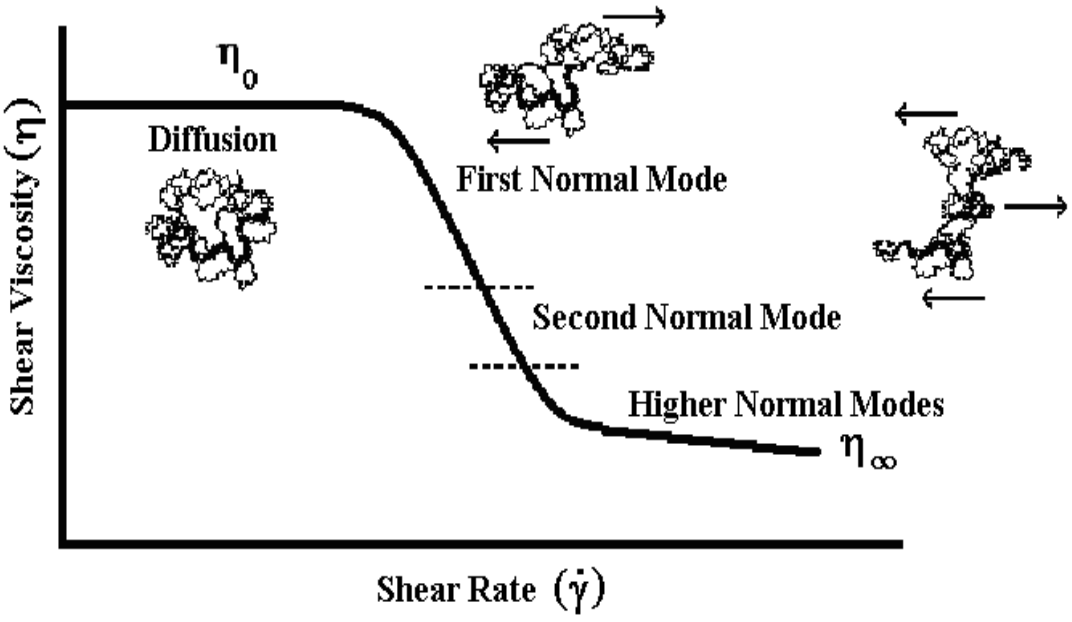

Figure 7. Plot showing change in shear viscosity as a result of increasing shear rate with modes for an isolated polymer molecule shown.

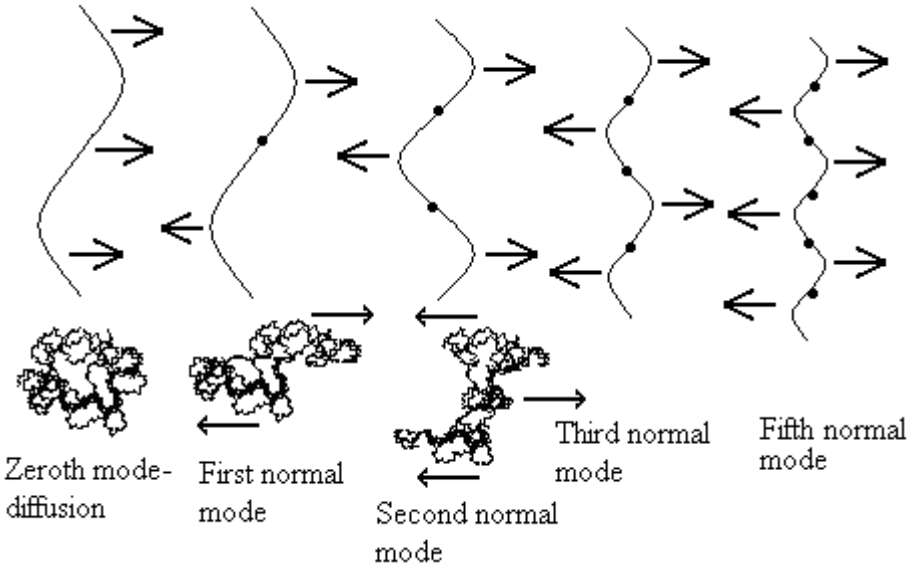

Figure 8. Diagram of the normal modes of vibration of a polymer chain.

Rouse theory can be used to describe the viscoelastic behaviour of linear low molecular weight polymer melts, where the behaviour is a function of the molar mass of the chain. When entanglement occurs at higher molecular weights, above M_c, a 'reptation' type motion can be used to describe the behaviour. This type of model is not appropriate for branched chain polymer systems building to form a network. This type of behaviour is observed in the melt phase of high molecular weight polymers. In order to model the cure of an epoxy resin, modified equations are required to predict both types of behaviour.

In the case of cure the initial stages of the process resemble those of the growth of a polymer in a solvent (the monomer) and the creation of a state which resembles a polymer melt. However as the cure reaction proceeds a monomer will be consumed and the liquid will be converted to a solid. The liquid is said to have vitrified and the viscosity has become very large, essentially infinite. In the case of a system which can undergo crosslinking the transition from the liquid to a solid may involve the creation of a rubbery network which will continue to cure and form a glassy state.

DryAdd [5] is a commercial software program, based on Monte Carlo simulations, that gives the connectivity of each monomer to another monomer in the system. The

output of the DryAdd programme provides information on the topography of the polymer chains as they grow. After the initial creation of short chain linear polymers, the growth will create branched chain molecules. The point along the chain at which branches occur must be nodes for the dynamic motion of the polymer chain. The following equations [6] are utilised in order to model the cure of an epoxy resin- from low molecular weight species to densely cross-linked polymers.

Instead of examining the shear modulus it is useful to consider the inverse which is termed the compliance. The term $J^*(\omega)$ is the compliance and is a relaxation component described by a Davidson-Cole type function with the following form (where η_0 is the low frequency limiting value of the viscosity; J_0 is the magnitude of the relaxing component of the compliance; J_∞ is the high frequency limiting value of the compliance; τ_r is the longest retardation time of the process; and β is a distribution function that describes the width (skewness) of the retardation process:

$$J^*(\omega) = J_\infty + \frac{1}{i\omega\eta_0} + \frac{J_0}{(1+i\omega\tau_r)^\beta}$$

Equation 2.3

This equation describes the frequency dependence in terms of a simple relaxation process which describes the simple relaxation of a Newtonian liquid. Using this definition of the compliance, the high frequency modulus $G^*(\omega)$ for simple liquids and low molecular weight polymers with molar mass below M_c can be described using the following equation:

$$G^*(\omega) = \frac{1}{J^*(\omega)}$$

Equation 2.4

For low molecular weight polymers and simple liquids the associated relaxation time is dependent on whole molecule rotation. However, in oligomers, internal rotations affect the relaxation time and Equation 2.3 can be modified as follows (where the Maxwell relaxation time $\tau_M = \eta J_\infty$):

$$J^*(i\omega) = J_\infty\left[1+\frac{1}{i\omega\tau_M}\right]+\frac{J_e}{(1+i\omega\tau_r)^\beta}$$

Equation 2.5

where J_e is the equilibrium limiting value of the relaxation contribution associated with the process. In the reaction system there will be two contributions to the relaxation - one from the unreacted monomer and the second from the growing polymer chains. The equilibrium compliance is the sum of two components, J_∞ and $J_{r,}$ where J_∞ is that of the liquid and J_r the contribution associated with the growing polymer and assuming that the relaxation has the Debye ideal form $\beta = ½$. It will be assumed that J_∞ is equal to J_r and Equation 2.5 then becomes as follows:

$$J^*(i\omega) = J_\infty\left[1+\frac{1}{i\omega\tau_M}\right]+\frac{2J_\infty}{(1+i\omega\tau_M)^{1/2}}$$

Equation 2.6

By measuring J_∞ and η it is possible to describe the behaviour of a low molecular weight polymer. The software package assumes that Equation 2.6 is applicable until the appearance of the first normal mode, and the limiting effective low frequency value η_0 is assumed to correspond to the highest normal mode of the polymer chain.

The Rouse model of the growing polymer chain can be used to describe a polymer melt that has *N* freely jointed segments with a molar mass below M_c. The frequency dependent behaviour can then be described as follows (where the τ values are the relaxation times of a series of *N* modes):

$$G^*(\omega)_{Rouse} = \frac{\rho RT}{M}\sum_{j=1}^{N}\frac{i\omega\tau_j}{1+i\omega\tau_j}$$

Equation 2.7

The relative τ values are given by the eigen-values of the *N* x *N* matrix *A* where:

$$A = \begin{vmatrix} 1 & -1 & 0 & 0 & ... & 0 & 0 & 0 \\ -1 & 2 & -1 & 0 & ... & 0 & 0 & 0 \\ 0 & -1 & 2 & -1 & ... & 0 & 0 & 0 \\ ... & ... & ... & ... & ... & ... & ... & ... \\ 0 & 0 & 0 & 0 & ... & -1 & 2 & -1 \\ 0 & 0 & 0 & 0 & ... & 0 & -1 & 1 \end{vmatrix}$$

If the polymer chain were a linear polymer then the matrix would become a simple diagonal matrix and Equation 2.7 would conform to the simple Rouse theory. However, because the chain is branched there are introduced a number of nodes designated by the off diagonal elements in the matrix.

The absolute value of the largest value is given by the following equation, where ζ_0 is the monomer friction coefficient, N_a is Avogadro's number, m_0 is the repeat unit weight, R is the gas constant, T is the absolute temperature and M is the molecular weight:

$$\tau = \left(\frac{\zeta_0 \, N_a}{\pi \, m_0 \, RT} \right) M^2$$

Equation 2.8

When the molar mass is above Mc the effects of chain entanglement or reptation must be taken into account. The reptation motion of an entangled polymer chain can be described by Equation 2.9, where G_0 is the terminal modulus corresponding to the value in the tail of the relaxation and T_d is the terminal relaxation time as defined in Equation 2.10.

$$G^*(\omega) = \frac{G_0}{5} \sum_{j=1}^{\infty} \left(\frac{8}{j^4 \, \pi^2} \right) \frac{T_d}{1 + \left(i\omega T_d / j^2 \right)}$$

Equation 2.9

$$T_d = \frac{5\pi^2 \eta(0)}{8G_0} \sum_{j_{odd}} \frac{1}{j^4}$$

Equation 2.10

It is further assumed in the software that the modulus terms are additive, at least for relatively low molecular weight materials for which the reptation contribution is very small. The total modulus of the system becomes:

$$G^*(\omega) = G^*_{reptation}(\omega) + G^*_{Rouse}(\omega) + G^*_0(\omega)$$

Equation 2.11

The above theory has been shown to be useful to relate the topography to the viscosity change which occurs during cure. While useful for consideration, and for understanding the relationships, the systems studied within this thesis have not been modelled using the DryAdd software.

2.1.4 Strathclyde Curemeter

The Strathclyde Curemeter is a vibrating needle rheometer that was developed by the physical chemistry department of Strathclyde University, and is used to investigate the rheology of various polymeric systems [7, 8].

This instrument is used in preference to conventional rheological measurements using conventional methods (e.g. capillary, rotational and vibrational (oscillatory) rheometers) when the materials are either highly filled or cure to form a solid mass. Conventional rheometers can be damaged if used to study curing systems. Vibrating probe methods can be more easily used as the probe is driven by a simple spring. When the cure has finished the probe can be removed easily and either stripped of epoxy or discarded. Also, when following the cure of an epoxy resin it is necessary to use an instrument that can monitor over a range of approximately 10^{-2} to 10^{6} Pa s, and vibrating probes are more suited to this range than conventional ones.

The Strathclyde curemeter allows the changes which occur going from a monomer to a gel to a vitrified solid to be followed using a single experiment. The instrument is based upon a vibrating paddle which has small dimensions typically 3 mm^2 and is connected to a constant amplitude and constant frequency linear motor by a spring. See Figure 9 below for a schematic diagram, where LVDT is the linear variable

differential transformer (a displacement transducer that works using a differential transformer) that monitors the motion of the probe. The output from the LVDT is a signal that indicates the amplitude and phase of the vibration of the paddle which is dipped into the fluid under investigation. When the instrument was first developed a range of frequencies and amplitudes were investigated and it was found the optimal values for most systems were a frequency of 2 Hz, and an amplitude of 1 mm.

The oscillating paddle is inserted into the uncured resin sample and the cure followed through viscosity changes. The amplitude and phase of the motion at the bottom of the spring are directly related to the degree of dampening produced by the curing sample as the viscosity builds up. The sample is mounted in a temperature block that allows isothermal heating. This system can monitor cure over the range 10^0 to 10^5 Pa s.

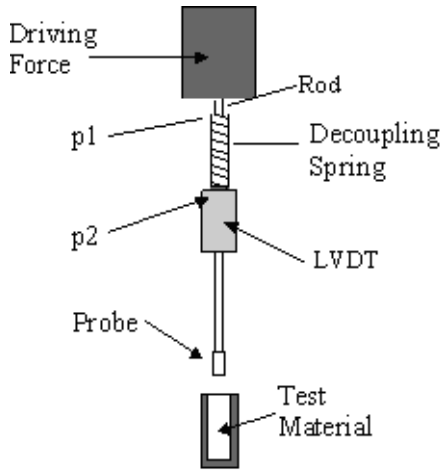

Figure 9. Schematic of the Strathclyde Curemeter design.

The assumptions associated with the design of the curemeter are [8]:

- The mass of the probe is negligible, i.e. resonant behaviour of the probe/ spring can be neglected.
- The change in the probe to material contact area with probe movement is negligible.
- The force on the probe due to the material is only based on viscous drag, i.e. no elastic forces or stirring of the material occur.

The forces at the lower end of the coupling spring, due to dampening as cure proceeds, can be written as:

$$k(p_1(t) - p_2(t)) + \eta C \frac{dp_2(2)}{dt} = 0$$

Equation 2.12

where k is the spring constant, p_1 and p_2 are the instantaneous displacements from equilibrium at points 1 and 2 respectively, η is the shear viscosity of the material at the frequency of the oscillation, and C is a geometric factor related to the probe/material contact area.

Since $p_1(t)$ is a sinusoidal function, the differential equation can be written in complex notation as follows (where p_1 and p_2 are respectively the amplitudes of the motor either side of the spring, η may be complex but is assumed to be simple, and ω is the frequency of the oscillation):

$$k(p_1 - p_2) + i\eta\omega C p_2 = 0$$

Equation 2.13

Assuming that η is purely real, the 'real' (p_2') and 'imaginary' (p_2'') components of p_2 can be equated as:

$$p_1 - p_2' - \left(\frac{\eta\omega C}{k}\right) p_2'' = 0$$

Equation 2.14

and

$$p_2'' - \left(\frac{\eta\omega C}{k}\right) p_2' = 0$$

Equation 2.15

Thus, solving for the 'real' (p_2') and 'imaginary' (p_2'') components gives:

$$p_2' = \frac{p_1}{1 + \left(\eta\omega C / k\right)^2}$$

Equation 2.16

and

$$p_2'' = \frac{p_1 \eta \omega C / k}{1 + \left(\eta \omega C / k \right)^2}$$

Equation 2.17

The resultant data can be viewed using the software program PicoLog, and is shown as the 'real' and 'imaginary' component plots, where the real component is the in phase motion of the probe, and the imaginary component is the out of phase component. The amplitude plots can be converted to viscosity plots and from these the activation energy for the gelation process can be calculated by using the time taken to gel, where the arbitrary viscosity value of 10^4 Pa s is used. Many studies of the cure of resins have shown that gelation occurs around a value of the viscosity reaching 10^4 Pa s – this being the point at which G' and G" cross over. Other researchers have used alternative arbitrary values, the imaginary peak maximum, the value half way down the real curve, or the intersect of the real and imaginary curves to give a time to gelation and hence a rate. An example plot for the reaction between a bisphenol-A-based epoxy resin and an amine curing agent is shown in Figure 10 below, where the black and red lines in the amplitude plot are the real and imaginary components respectively. The viscosity plot obtained from the curemeter differs from that shown in Figure 6 in that the initial (horizontally linear) Newtonian region is masked by instrumental noise.

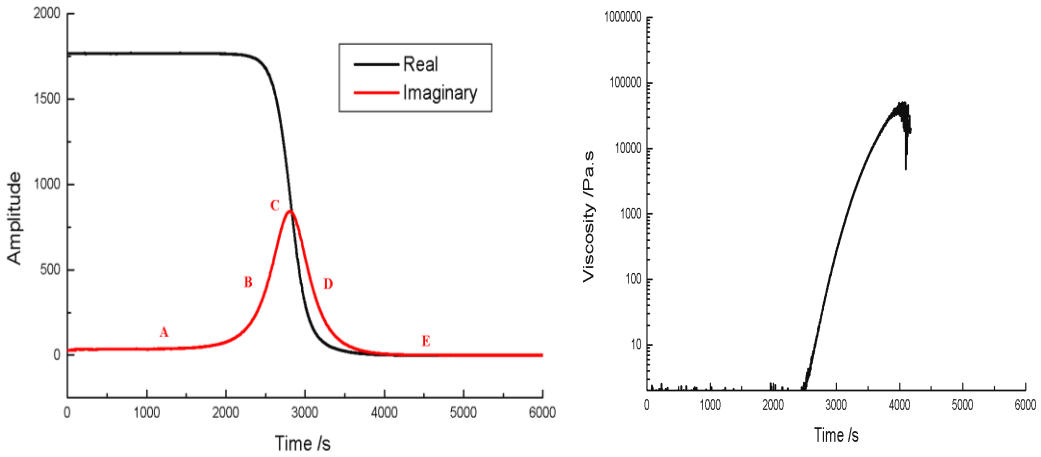

Figure 10. Example plots from Strathclyde Curemeter where the left hand plot shows a typical amplitude trace and the one on the right shows the amplitude data converted to a viscosity plot.

The out of phase (imaginary) curve gives an indication of the changes which occur in the system as cure occurs. In region A (marked in Figure 10) the curing system has a low viscosity and the liquid is purely Newtonian, with the curing material being constituted from monomer, dimer and low molar mass species. As cure progresses so the molar mass of the species present increases and the liquid starts to gain viscoelastic characteristics. In region B the phase shift indicates that the liquid has gained a degree of elasticity. The maximum in the degree of elasticity will occur at region C and this may be considered to coincide with the point at which a network is formed throughout the liquid. Beyond region C, the material is becoming more rigid and the effect is that the energy which can be dissipated is decreased as in a reduction in amplitude in region D. When a rigid solid is formed the probe ceases to oscillate and at region E the system has vitrified and formed a glassy solid. In terms of the critical points on the phase curve which define a curing system, region C can be associated with gelation, and region E with vitrification.

2.2 DIFFERENTIAL SCANNING CALORIMETRY (DSC)

Differential Scanning Calorimetry (DSC) measurements can provide qualitative and quantitative information about the chemical and physical changes (that involve endothermic, exothermic processes or changes in heat capacity) in a sample by measuring the heat flow associated with transitions in the material as a function of time and temperature. The method can provide information about several events (e.g. glass transitions, melting and boiling points, crystallisation/crystallinity, heats of fusion and reactions, specific heat and heat capacity), as well as information about oxidative stability, rate/degree of cure, reaction kinetics, purity and thermal stability [9]. The difference in the heat flow into or out of the sample and a reference (an empty pan) is used to provide this information. As the empty reference pan cannot have a thermal event associated with it, the instrument adjusts the input of heat (or cooling) to the sample pan accordingly, thus the temperature of each is kept the same (i.e. $\Delta T=0$). The specific heat capacity of the sample is plotted against the temperature (or the time), and the temperature at which thermal events (e.g. glass

transition, melting) occur can be read directly from the plot, assuming that the instrument has been calibrated [10-14].

DSC can be used to estimate Arrhenius kinetic parameters, e.g. Activation Energy (E_a), pre-exponential term (A), rate constant (k) and the reaction order (n) [9, 14]. Hadad [14] stated that the assumption that the exothermic heat evolved during cure is proportional to the extent of reaction must be made. TA Instruments, the manufacturers of the DSC instrument used for this study, investigated three methods for DSC kinetic studies [15, 16]: Borchardt and Daniels (dynamic); ASTM E-698 Thermal Stability (dynamic scans using three or more different heating rates); and isothermal (the sample is held at a temperature for a set length of time). They reported that the isothermal method was preferable for n^{th} order and autocatalytic reactions or for the investigation of a new reaction (where the reaction mechanism is unknown). It has been stated that although the isothermal method has longer scan times, it often produces more reliable kinetic parameters than the other approaches, as fewer experimental variables are introduced so data interpretation is easier with less ambiguity over results [15-17]. Hadad [14] reports that when the isothermal heat of reaction (ΔH_{iso}) is found by doing an isothermal scan of the material as it cures and integrating to find the area under the cure; and dynamic scans are done after each isothermal scan to determine the residual heat of reaction (ΔH_{res}); then the total heat of reaction (ΔH_{total}) is the sum of the two components; and the degree of conversion is found as follows:

$$\alpha = \Delta H_{iso} / \Delta H_{total}$$

Equation 2.18

TA Instruments suggest obtaining the total heat of reaction by doing a dynamic scan of the uncured material, and then calculating the degree of conversion as in the equation above. Plotting α against time will give conversion plots and the rates from these could be used to draw an Arrenhius plot and thus find the activation energy of initiation.

2.3 FOURIER TRANSFORM INFRA-RED (FT-IR) SPECTROSCOPY

Infra-red (IR) spectroscopy is commonly used to monitor the cure of epoxy resins, as functional groups have characteristic vibrational frequencies, e.g. the epoxy group can be found at ca. 914-917 cm^{-1}. Fourier transform infra-red (FT-IR) spectroscopy offers advantages over dispersive IR as a whole spectrum (typically 5000-400 cm^{-1}) can be measured in a few seconds, with high resolution and good sensitivity [12, 18]. This allows the spectrum of a thin film of curing epoxy to be measured at pre-determined time intervals, and quantitative as well as qualitative information can be determined [14]. In order to overcome instability in the instrument, the C-H absorption at *ca.* 3000 cm^{-1} was used as an internal standard.

The cure can be followed quantitatively by using the ratio of the epoxy absorbance band (or some other band of a component of the reaction that changes) to a reference band (that does not change throughout the cure) [14], and if the ratio at the start of cure and after some time interval can be calculated, the degree of conversion α can be calculated as follows, where A is the absorbance of the band in cm^{-1}, t is the time and t_0 is the initial time:

$$\alpha = \frac{A_{REACTIVE\ (t)}}{A_{REFERENCE\ (t)}} \Bigg/ \frac{A_{REACTIVE\ (t_0)}}{A_{REFERENCE\ (t_0)}}$$

Equation 2.19

If the cure is carried out at a range of temperatures, an Arrhenius plot could be drawn using the rates from the plots of α *vs*. time, and from this the activation energy calculated.

To obtain accurate measurements it is very important that the temperature of the cell is controlled precisely and that the instrument is stable over the long time period required for the measurement. An important difference between the spectroscopic observations and those of the rheology and DSC is the size of the sample being studied. Thin films are required in order to achieve the required transparency of the sample for FT-IR, and as a result there would be less tendency for the sample to

exotherm compared with a situation where larger/thicker samples are used. It is important to understand this difference when interpreting and comparing the data later in the thesis.

2.4 DIELECTRIC SPECTROSCOPY

Dielectric spectroscopy has been used for many years to monitor the cure of epoxy resins as it is a non-invasive, and hence non-destructive, technique. It is a form of relaxation spectroscopy and makes use of the polar nature of epoxies. When polar materials are placed in an alternating electric field of variable frequency, i.e. in between two parallel conducting plates, the permanent electric dipoles in the molecule try to line up parallel to the field direction. The mobility of the dipoles within the system will determine their ability to align, and so using the technique can give information on molecular transitions, physical properties and the heterogeneity of the system.

2.4.1 Dielectric Polarisation in an Alternating Field

If the field is small and alternating, the dipoles will be forced to realign and a current will be produced. Hadad [14], in agreement with Campbell and White [12], reports that the dipole movement is restricted by internal friction causing some electrical energy to be lost as heat, resulting in a loss current that is 90° out of phase with the charge current. They go on to state that the dipole realignment can be related to the rheology of the resin as it becomes increasingly difficult for the dipoles to align as the cure proceeds because of steric constraints and internal friction. When the material is fully cured, it will be cross-linked and rigid, so the dipoles will be mainly immobile. Cowie [10] states that the complex dielectric permittivity ε^* can be measured from the change in amplitude, and that it can then be resolved into its two components if the change in current described above is known. The components are ε', the dielectric permittivity (storage), and ε'', the dielectric loss, and are respectively related to changes in the dipolar activity and the conductivity. The dielectric permittivity can be thought of as the energy that is stored per cycle, and is often

referred to as the *real* permittivity. The dielectric loss can be thought of as the energy dissipated per cycle, and is referred to as the *imaginary* permittivity. The three terms are related as shown in the equation below:

$$\varepsilon^* = \varepsilon' - i\varepsilon''$$

Equation 2.20

2.4.2 The Debye Equations

Cowie [10] states that the dielectric relaxation processes can be described by the following Debye relaxation equations:

$$\varepsilon' = \varepsilon_\infty + \frac{(\varepsilon_s - \varepsilon_\infty)}{1 + \omega^2\tau^2}$$

Equation 2.21

$$\varepsilon'' = \frac{(\varepsilon_s - \varepsilon_\infty)\omega\tau}{1 + \omega^2\tau^2}$$

Equation 2.22

where ε_s is the static dielectric constant related to actual dipole moment of the polymer and where all dipoles have sufficient time to re-align; ε_∞ is the instantaneous dielectric permittivity, which is measured at high frequencies to allow insufficient time for dipole re-alignment, so ε_s - ε_∞ is a measure of the strength of the molecular dipole involved in the relaxation that occurs; ω is the angular frequency of the applied field; and τ is the relaxation time which can also be written as $1/\omega_{max}$.

This can then be simplified to give the Debye equation for the complex dielectric permittivity:

$$\varepsilon^* = \varepsilon_\infty + \frac{(\varepsilon_s - \varepsilon_\infty)}{1 + i\omega\tau}$$

Equation 2.23

The ratio of dielectric constant and loss is termed the dielectric loss tangent, or the dissipation factor, tan δ:

$$\tan\delta = \frac{\varepsilon''}{\varepsilon'}$$

Equation 2.24

A maximum in the tan δ can be useful in examining the dielectric data as it can be correlated to the T_g, and an Arrenhius equation exists between the time to the tan δ maximum and the temperature, allowing the activation energy to be calculated [10-12, 14].

The cure progress can also be related to the relaxation time τ which is found when the dielectric loss factor passes through a characteristic maximum frequency (ω_{max}), and τ is equal to the reciprocal of that frequency. When the frequency is above ω_{max} both the storage and loss components are low as the dipoles do not move quickly enough to follow the alternating field. When the frequency is below ω_{max} the storage component is high as the dipoles are in alignment with the field, and the loss is low due the current being out of phase with the voltage [10, 14]. The relationship between ε′, ε″, ω_{max}, and tan δ is summarised in Figure 11. The processes are temperature dependent and as the temperature is increased the observed relaxation will shift to lower frequencies. It is important to recognise that the point at which tan δ reaches a maximum does not coincide with the maximum in the dielectric loss – the former being shifted relative to the latter as a consequence of the drop in the value of the dielectric permittivity. Whilst the maximum in the tan δ is often used to identify the location of the T_g process it does not coincide exactly with the maximum in the loss which is the point at which the dipolar motion matches the condition the relaxation time, τ, is equal to the reciprocal of the angular frequency of the applied field. This is the relationship that connects the molecular mobility with the bulk dielectric observation.

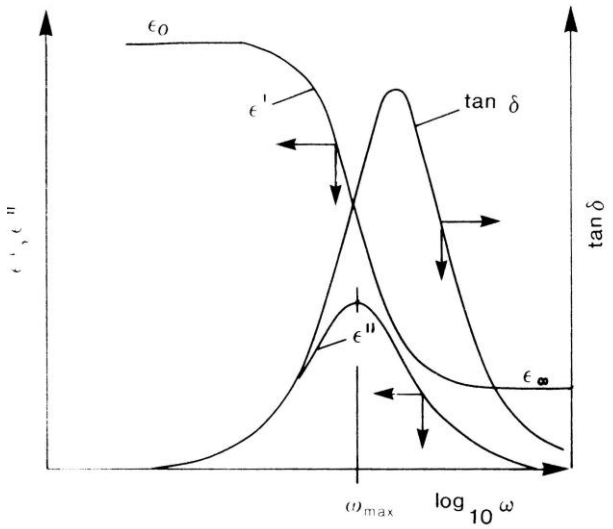

Figure 11. ε′, ε″ and tan δ as a function of angular frequency for a molecular relaxation [19].

2.4.3 Dielectric Response of Polymers

The loss profile of solid polymeric materials is not as simplified as shown in Figure 11, as different molecular motions result in several distinct relaxation processes occuring at different temperatures and frequencies, and these relaxations are termed α, β, γ… *etc*. Figure 12 shows the dielectric loss curve for a solid polymeric material at constant frequency against temperature, where the α-relaxation is that of the loss peak in Figure 11.

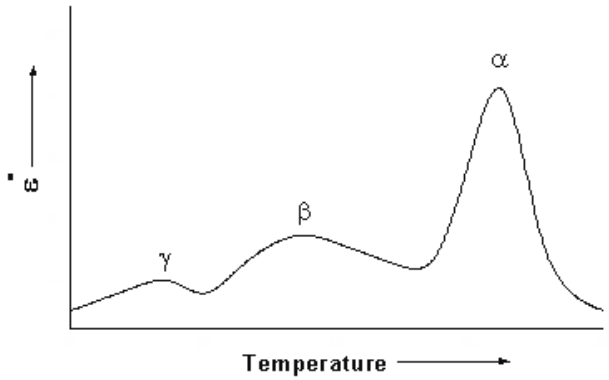

Figure 12. Dielectric loss curve for a solid polymeric material at constant frequency showing α, β and γ relaxations [20].

The α-relaxation is associated with the increased ability of the permanent dipoles attached to the polymer backbone to rotate in the electric field. The physical rotation of a main chain segment requires co-operative motion from neighbouring segments,

and so the α-relaxation occurs when there is an increase in the free volume of the system, *i.e.* when there is sufficient freedom of movement. This correlates with the amorphous polymers' glass transition temperature range. As well as α-relaxations, there are usually β-processes that are associated with independent side/pendant group rotations, and these occur at lower temperatures.

Real polymer materials are generally not simple homogenous systems that can be described by one specific relaxation time as given in the Debye model. Relaxations in polymers tend to display broader dispersion curves and lower loss maxima than simple polar liquids. Cole and Cole [21] modified the Debye equation for the complex dielectric permittivity (Equation 2.23) by introducing the α-term, as shown in Equation 2.25 (where $0 < \alpha \leq 1$):

$$\varepsilon^* = \varepsilon_\infty + \frac{\left(\varepsilon_s - \varepsilon_\infty\right)}{1+\left(i\omega\tau\right)^{1-\alpha}}$$

Equation 2.25

For an ideal Debye relationship the resulting plot of the ratio, termed a Cole-Cole plot, should be a perfect semi-circle (symmetrically distributed about τ) with α=1 (Figure 13). The plots act as a good visual aid to check how far data from a real polymer system is from fitting the ideal relationship. The relaxation values become more disperse with decreasing α values. The orientation of segmental dipoles is restrained by the entanglement of long chain molecules and so a disperse range of permittivities is produced.

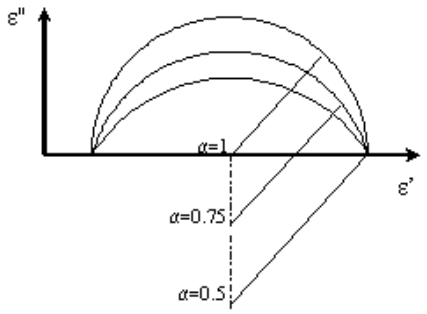

Figure 13. Cole-Cole plot for an ideal Debye relationship generated by plotting the real and imaginary dielectric constants against each other, and showing the result of varying α [20].

The Cole-Cole modification was improved upon by Cole-Davidson [22] to include a β-term, and to give the semi-empirical equation (where $0 < \beta \leq 1$):

$$\varepsilon^* = \varepsilon_\infty + \frac{(\varepsilon_s - \varepsilon_\infty)}{(1 + i\omega\tau)^\beta}$$

Equation 2.26

The β-term has the effect of skewing the Cole-Cole arc as shown in Figure 14.

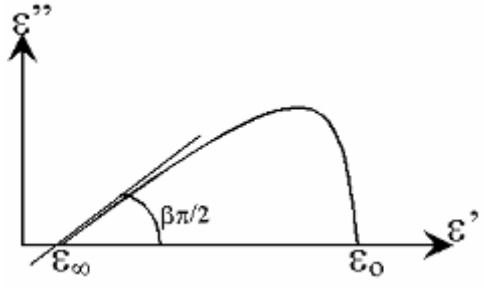

Figure 14. Cole-Davidson plot generated by plotting the real and imaginary dielectric constants against each other, where the β-term has the effect of skewing the Cole-Cole arc [20].

The Havriliak-Negami (H-N) relaxation is a combination of Cole-Cole and Cole-Davidson equations, and accounts for asymmetry and the broadness of the curve by adding both of the parameters α and β as follows [23]. An example H-N plot is show in Figure 15.

$$\varepsilon^* = \varepsilon_\infty + \frac{(\varepsilon_s - \varepsilon_\infty)}{\left(1 + (i\omega\tau)^{1-\alpha}\right)^\beta}$$

Equation 2.27

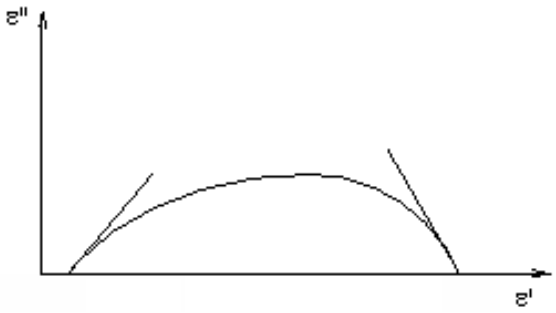

Figure 15. Example Havriliak-Negami plot produced by plotting the imaginary against the real dielectric constant, and where both the α and β parameters affect the curve shape [20].

The H-N modification allows the experimental data to be fitted to empirical curves and parameters such as α and β to be extracted and plotted as a function of time and/or frequency. Other parameters that can be modelled include: $\Delta\varepsilon$, ε_∞, σ and ω_{max}. As the isothermal curing temperature is changed characteristic trends should emerge for these parameters that can then be incorporated with the experimental data from other cure characterisation methods to produce Time-Temperature- Transformation (TTT) diagrams.

2.4.4 Dielectric Response of Heterogeneousc Polymers

The previous equations are only true for one-phase systems, *i.e.* the simple polymer. When a second phase such as unreacted monomer, ionic species (chlorine is often present in epoxies as an impurity) or water is present the system becomes multi-phase, and hence heterogenic. The heterogeneity of real polymer systems can significantly alter the measured permittivity, and in particular additional loss processes can occur at lower frequencies compared to the relaxations described above. These interfacial polarisation processes occur at the interface of the main polymer and the heterogeneous particles and are a result of a build-up of virtual charges. They are often termed Maxwell-Wagner-Sillars (MWS) effects, and changes in the position, size and shape of the MWS loss can be used to investigate morphological changes in the sample being studied.

The following equations are for a simple two phase system which has layers 1 and 2, each with a permittivity ε, conductivity σ and thickness d [24]. Where there is no numerical subscript to denote the particular phase a bar is used above the symbol to indicate that these equations are MWS approximations of the Debye equations. In this way the static permittivity ($\bar{\varepsilon}_s$), instantaneous permittivity ($\bar{\varepsilon}_\infty$) and conductivity of the system ($\bar{\sigma}$) as well as the relaxation time for the MWS process (τ_{MW}) are defined in the following equations. The overall sample thickness d is equal to $d_1 + d_2$.

$$\bar{\varepsilon}_s = \frac{d\left(\varepsilon_1' d_1 \sigma_2^2 + \varepsilon_2' d_2 \sigma_2^2\right)}{\left(\sigma_1 d_2 + \sigma_2 d_1\right)^2}$$

Equation 2.28

$$\bar{\varepsilon}_\infty = \frac{d\varepsilon_1' \varepsilon_2'}{\varepsilon_1 d_2 + \varepsilon_2 d_1}$$

Equation 2.29

$$\bar{\sigma} = \frac{d\sigma_1 \sigma_2}{\sigma_1 d_2 + \sigma_2 d_1}$$

Equation 2.30

$$\tau_{MW} = \varepsilon_0 \frac{\varepsilon_1' d_2 + \varepsilon_2' d_1}{\sigma_1 d_2 + \sigma_2 d_1}$$

Equation 2.31

where ε_0 is the permittivity of free space ≈ 8.854 x 10^{-12} F m^{-1}.

These terms can then be applied to the Debye equations to give the overall real and imaginary permittivity components as follows:

$$\varepsilon'(\omega) = \bar{\varepsilon}_\infty + \frac{\bar{\varepsilon}_s - \bar{\varepsilon}_\infty}{1 + \omega^2 \tau_{MW}^2}$$

Equation 2.32

$$\varepsilon''(\omega) = \bar{\varepsilon}_\infty + \frac{\left(\bar{\varepsilon}_s - \bar{\varepsilon}_\infty\right)\omega\tau_{MW}}{1 + \omega^2 \tau_{MW}^2} + \frac{\bar{\sigma}}{\omega}$$

Equation 2.33

The loss component therefore has an additional term for the conductivity of the sample. There are further equations to describe systems with more than two layers, however these will not be discussed within this work.

The effect of water ingress into an epoxy resin and the resultant dielectric response will be dealt with in *Section 2.5.2*.

2.4.5 Dielectric Response During Epoxy Resin Cure

Dielectric spectroscopy provides an indirect measure of the viscosity and so can be a useful non-destructive testing method. Most commercial curing systems contain small quantities of ionic species such as Na^+ and Cl^- which are left over from the synthesis. The translational movement of these ions will dominate the dipolar molecular response when the system is in its early liquid state. As the ionic movement is closely related to the viscosity, this motion can be used in cure monitoring. The observed relaxation due to the increasingly immobile dipoles will shift down the frequency range as the cure proceeds, and the dc conductivity contribution (to the imaginary permittivity) will disappear to lower frequencies. The initial dielectric response is that of the monomers and these will be able to relax at frequencies above 10^7 – 10^8 Hz. As the molecular weight increases the dipole relaxation will be slowed down and will fall below 10^5 Hz. As the glass state is approached, the ions become so immobile that the molecular dipolar response of the molecules becomes detectable. Usually at this stage the network is sufficiently well developed that the only relaxation of the dipoles possible will involve side chain motions of the pendant hydroxyl groups created by epoxy ring opening and to a much lesser extent the reorientation of the ether dipole associated with the phenyl ring. These pendant hydroxyl groups on the main chain will be able to exhibit β type relaxations once the material has passed through its glass transition temperature.

2.5 MOISTURE INGRESS

2.5.1 Moisture Ingress into Cured Epoxy Resins

Water is known to enter epoxy resins by diffusion through the adhesive and also capillary action through voids and cracks incorporated into the material upon cure. Water ingress into resins and composites is one of the major factors associated with the deterioration of materials when they are subjected to environments that contain a high level of moisture. Epoxies have a high affinity for water, absorbing up to 20% of their own mass, and this is due to the high number of potential sites available for hydrogen bonding along the polymer chain (diffusion) and the number of voids in the

structure (capillary action) [20]. Once absorbed, the water causes a reduction in the T_g and the modulus resulting in decreased mechanical properties [25]. Also, water ingress may result in hydrolysis of the resin leading to main chain scission which then causes an increased susceptibility to further chemical attack [26].

There are several factors which affect the rate of diffusion of water into an epoxy. The first and likely to be the largest is the ageing temperature which causes an increase in absorption with increasing temperature. However, above the T_g, the system has enough energy to allow molecular rearrangement and so water molecules can diffuse more easily and the process is not time-dependent. Below the T_g, the rate of diffusion is faster than the rate of molecular rearrangements and so diffusion rates are then related to the free volume of the system. The second factor that affects diffusion is the physical and chemical structure of the epoxy, where increasing the mobility of the chains and creating free volume, or the presence of polar groups, increases the diffusion rate. Crystalline or locally ordered regions and high degrees of cross-linking decrease diffusion by restricting the mobility of the chains [20].

Water ingress into a polymer can be described using Fick's laws of diffusion. The first law states that the flux of a substance by diffusion in the direction x is proportional to the gradient of concentration in that direction:

$$F = -D\frac{\partial C}{\partial x}$$

Equation 2.34

where F is the rate of mass transfer per unit area of section (i.e. flux), C is the concentration of the diffusing substance (e.g. water), x is the space coordinate and D is the diffusion coefficient (constant).

The equation is based on the assumption that the rate of transfer of diffusing matter (water) through the unit area is a result of random molecular motion and is proportional to the concentration gradient. Crank and Park [27] state that if F and C are both expressed in the same unit of quantity (e.g. gram or gram molecules) then D

can have dimensions: length^2 time^{-1}, i.e. cm^2 s^{-1}. Fick's second law of diffusion is described by the equation:

$$\frac{\partial C}{\partial t} = D\frac{\partial^2 C}{\partial x^2}$$

Equation 2.35

This second law only applies for two component systems where the mixture is incompressible (liquid or solid phase) and where no volume change occurs on mixing. Crank and Park [27] state that it must be assumed that there is a concentration gradient in one direction only, e.g. along the x-axis. When a diffusion process can be described by either of these laws the process is said to be 'Fickian Diffusion'.

Diffusion of moisture into cured epoxies is generally thought to obey Fick's second law and the equations below can be derived to allow determination of the diffusion coefficient, D [28]. Most calculations of D that use gravimetric mass uptake data use a normalised expression for the change in mass, in order to take into account the initial mass of the sample. Therefore, the Boltzmann solution for the initial stage of diffusion is given as:

$$\frac{M_t - M_0}{M_\infty - M_0} = \frac{4}{\sqrt{\pi}}\sqrt{\left(Dt/l^2\right)}$$

Equation 2.36

where M_0 is the mass of the sample at time t = 0; M_t denotes the total mass of solvent which has entered the polymer (mass at time t); M_∞ denotes the corresponding mass at equilibrium (the final maximum mass) and is strongly dependent on the polarity of the cured resin (the more polar the resin, the higher the value of M_∞); l is the thickness of the material; and D is the diffusion coefficient.

The (gravimetric) diffusion coefficient can be determined from the initial gradient of the sorption curve given by plotting the change in mass (left hand side of the equation) against the square root of time divided by the thickness, as shown by the following equations:

$$D = \frac{\pi}{16} R^2$$

Equation 2.37

where R is given by:

$$R = \frac{d\left(M_t / M_\infty\right)}{d\left(\sqrt{t}/l\right)}$$

Equation 2.38

An example sorption curve, for an epoxy resin aged in water is given in Figure 16. For a process to be considered Fickian, there are two prominent features of a sorption curve which must be satisfied: at least 60% of the initial portion of the curve must be linear to allow the diffusion coefficient to be calculated, and above the linear section, the curve should be concave against the x-axis [20].

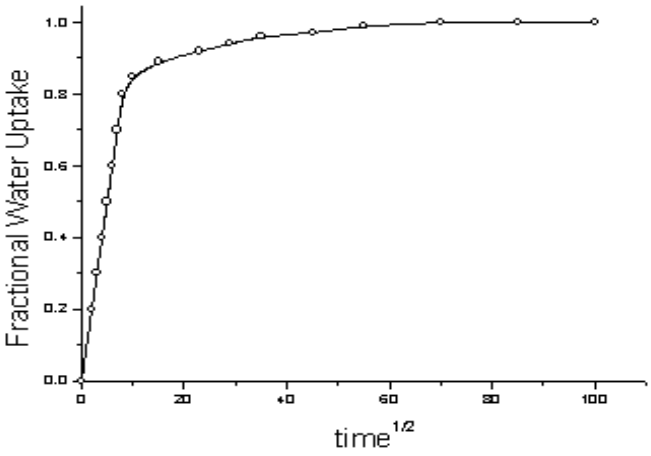

Figure 16. Sorption curve for an epoxy aged in water - showing Fickian type behaviour [20].

Where a material is studied below its T_g it may display non-Fickian type adsorption, and this can be classified according to the shape of the resultant plot [20]. Pseudo-Fickian curves are very similar to Fickian sorption curves except that the initial linear section is less than 60%. Two-stage adsorption curves have an initial stage that is similar to a Fickian sorption curve, and this stage is diffusion controlled. Swelling of the matrix then causes elastic forces to increase the chemical potential of the material (quasi-equilibrium) before they eventually decrease allowing the diffusion rate to

increase again until equilibrium is reached. An example two-stage adsorption plot is shown in Figure 17.

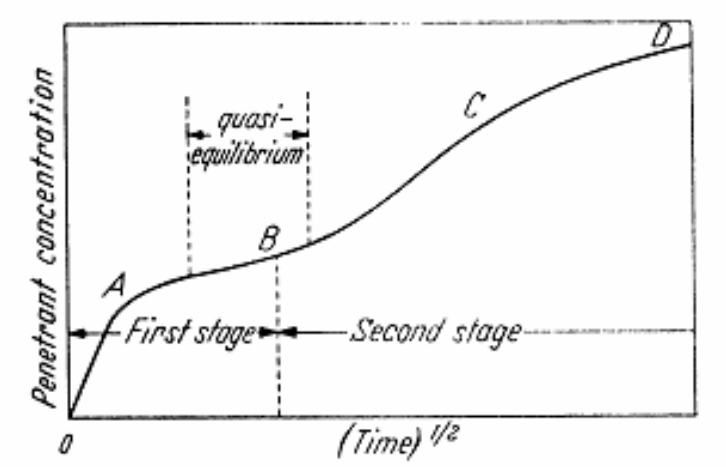

Figure 17. Example of a two-stage water adsorption curve [29].

2.5.2 Dielectric Response as a Result of Water Ingress

Moisture can exist in resins as *free* or *bound* water, and also as ice if the temperature is low enough, and all of these states will result in a dielectric response. It is generally agreed that for every 1% of water absorbed into an epoxy resin, the T_g is reduced by approximately 20 K due to plasticisation [28]. Figure 18 shows the main contributions that water makes to the dielectric loss: double layer effect (DL); ionic conduction (C); principle ice relaxation (I); crystal water relaxation (X); surface conductivity effect (S); Maxwell-Wagner-Sillars effect (MW); bound water relaxation (B); principle relaxation of free water (W1); and the secondary relaxation of free water (W2).

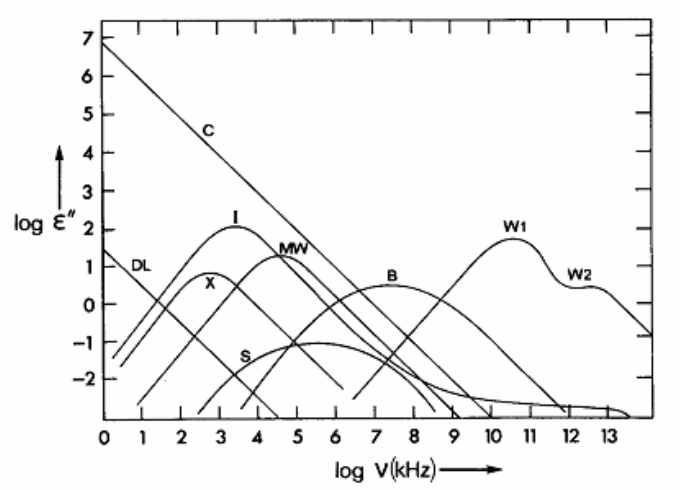

Figure 18. Plot showing the frequencies at which the main water relaxations in the dielectric loss occur [20].

When the three dimensional structure builds up micro voids (*ca.* 0.01 μm or less) may be formed as a result of a non-ideal cure schedule, *i,e.* when the cure temperature is high and the network is formed quickly, effectively locking reactive groups in so that they cannot react. The higher the cure temperature, the higher the void content of the cured resin and free water can be physically adsorbed into these cavities by capillary action. Water diffusing into the matrix can create osmotic pressure effects that result in the plasticised resin minimising the energy by the creation of void structure. It is therefore not unusual to observe that whilst the initial uptake of water occurs into an apparently homogenous matrix the characteristics may change to diffusion into a heterogeneous matrix as a consequence of the appearance of voids in the matrix. The free water contribution is associated with dipolar relaxation processes reportedly occurring above 10^6 Hz [30], as highlighted in Figure 18.

Water can become bound, through hydrogen bonding, to the tertiary amine nitrogen, ether oxygen, hydroxyl oxygen and hydroxyl hydrogen (where water acts as a hydrogen bond acceptor through the oxygen), as well as to other *free* water molecules within the matrix. All of these can lead to relaxations in the dielectric loss which occur at slightly lower frequencies than the *free* water. It has also been shown that the absorbed water can actually break up existing hydrogen bonds to form new ones with the polar groups in the polymer or matrix or the free water [31, 32].

Dielectric relaxation studies can monitor the uptake of water into the matrix and also provide information on the way it is distributed within the matrix.

2.6 CONCLUDING REMARKS

This chapter has considered the theory behind the experimental techniques employed in this work for cure characterisation: Rheology, Differential Scanning Calorimetry (DSC), Fourier Transform Infra-Red (FT-IR) Spectroscopy and Dielectric Spectroscopy. It has also considered the techniques employed for monitoring water ingress into epoxy resins.

2.7 REFERENCES

1. Barnes, H.A., J.F. Hutton, and K. Walters, *An Introduction to Rheology*. 1989, Oxford: Elsevier Ltd.

2. Goodwin, J.W. and R.W. Hughes, *Rheology for Chemists: An Introduction*. 2000: Royal Society of Chemistry: Cambridge.

3. Hudson, N.E., R.A. Pethrick, H.A. Barnes, and G.E. Eccelston, *Postgraduate Course: Process Rheology*. 2006, Strathclyde University.

4. Bailey, R.T., A.M. North, and R.A. Pethrick, *Molecular Motion in High Polymers*. 1981, Oxford: Clarendon Press.

5. *DryAdd polymerization and network modelling package, Version 3.1*, Oxford Materials Ltd., Chestnut Farm, Tarvin Road, Frodsham, Cheshire, UK.

6. Hayward, D., R.A. Pethrick, B. Eling, and E. Colbourn, *Prediction of the Rheological Properties of Reactive Polymer Systems.* Poly Int, 1997. **44**: p. 248-254.

7. Pethrick, R.A., *Chapter 3: Rheological Studies Using a Vibrating Probe*, in *Rheological Measurement*, A.A. Collyer and D.W. Clegg, Editors. 1998, Chapman & Hall: London.

8. Affrossman, S., A. Collins, D. Hayward, E. Trottier, and R.A. Pethrick, *A versatile method of characterising cure in filled reactive polymer systems.* Journal of the Oil & Colour Chemists Association, 1989. **72**(11): p. 452-454.

9. www.npl.co.uk/materials/cog/thermal.html. [cited.

10. Cowie, J.M.G., *Polymers: Chemistry & Physics of Modern Materials*. 2nd ed. 1991, London: Chapman and Hall.

11. Elias, H.-G., *An Introduction to Polymer Science*. 1997, Weinheim & New York: VCH.

12. Campbell, D. and J.R. White, *Polymer Characterization: Physical Techniques*. 1989, London: Chapman and Hall.

13. Walton, D. and P. Lorimer, *Oxford Chemistry Primers: Polymers*. 2000: Oxford University Press, Oxford.

14. Hadad, D.K., *Chapter 14: Physical and Chemical Characterisation of Epoxy Resins*, in *Epoxy Resins Chemistry and Technology*, C.A. May, Editor. 1988, Marcel Dekker, Inc.: New York & Basel.

15. Goodwin, A. and T. Lever, *TA-073: A review of DSC kinetics methods*. 2004, TA Instruments.

16. Goodwin, A. and T. Lever, *TA-143: A comparison of commercially available DSC kinetic methods for evaluating bismaleimide resins*. 2004, TA Instruments.

17. Waters, D.N. and J.L. Paddy, *Equations For Isothermal Differential Scanning Calorimetric Curves.* Analytical Chemistry, 1988. **60**(1): p. 53-57.

18. Williams, D.H. and I. Fleming, *Spectroscopic Methods in Organic Chemistry*. 5th ed. 1995, London: McGraw-Hill.

19. Blythe, A.R., *Electrical Properties of Polymers*. 1979, Cambridge: Cambridge University Press.

20. McConnell, B.K., *PhD Thesis: Dielectric Studies of Adhesively Bonded Structures*, in *Pure and Applied Chemistry*. 2006, University of Strathclyde: Glasgow.

21. Cole, K. and R. Cole, *Dispersion and Absorption in Dielectrics.* Journal Of Chemical Physics, 1941. **9**: p. 341-351.

22. Davidson, D. and R. Cole, *Dielectric Relaxation in Glycerol, Propylene Glycol and n-Propanol.* Journal Of Chemical Physics, 1951. **19**(12): p. 1484-1490.

23. Havriliak, S. and S. Negami, *A Complex Plane Representation of Dielectric and Mechanical Relaxation Processes in Some Polymers.* Polymer, 1967. **8**(4): p. 161-210.

24. Beek, L.v., *Chapter 3: Dielectric Behaviour of Heterogeneous Systems*, in *Progress in Dielectrics*, J.B. Birks, Editor. 1967, Heywood Books: London.

25. Boinard, E., R.A. Pethrick, J. Dalzel-Job, and C.J. MacFarlane, *Influence of resin chemistry on water uptake and environmental ageing in glass fibre reinforced composites-polyester and vinyl ester laminates.* Journal of Materials Science, 2000. **35**: p. 1931-1937.

26. Hasted, J.B., *Aqueous Dielectrics*. 1973, London: Chapman and Hall.

27. Crank, J. and G.S. Park, *Chapter 1. Methods of Measurement*, in *Diffusion in Polymers*, J. Crank and G.S. Park, Editors. 1968, Academic Press Inc. Ltd.: London.

28. Jones, F.R., *Chapter 8: Composite materials*, in *Chemistry and Technology of Epoxy Resins*, B. Ellis, Editor. 1993, Blackie Academic & Professional: Glasgow.

29. Fujita, H., *Diffusion in polymer-diluent systems.* Advances in Polymer Science, 1961. **3**(1): p. 1-47.

30. McEwan, I., R.A. Pethrick, and S.J. Shaw, *Water absorption in a rubber-modified epoxy resin; carboxy terminated butadiene acrylonitrile-amine cured epoxy resin system.* Polymer, 1999. **40**: p. 4213-4222.

31. Mijovic, J. and H. Zhang, *Molecular dynamics simulation study of motions and interactions of water in a polymer network.* Journal Of Physical Chemistry B, 2004. **108**(8): p. 2557-2563.

32. Mijovic, J. and H. Zhang, *Local dynamics and molecular origin of polymer network-water interactions as studied by broadband dielectric relaxation spectroscopy, FTIR, and molecular simulations.* Macromolecules, 2003. **36**(4): p. 1279-1288.